

Comparison of Drive-Seeded Modulations in Planar Foils for 0.35 and 0.53 μm Laser Drive

S. G. Glendinning,¹ S. N. Dixit,¹ B. A. Hammel,¹ D. H. Kalantar,¹ M. H. Key,¹ J. D. Kilkenny,¹ J. P. Knauer,²
D. M. Pennington,¹ B. A. Remington,¹ J. Rothenberg,¹ R. J. Wallace,¹ and S. V. Weber¹

¹Lawrence Livermore National Laboratory, University of California, Livermore, California 94550

²Laboratory for Laser Energetics, 250 East River Road, Rochester, New York 14623-1299

(Received 7 August 1997)

Laser-speckle-seeded modulations in laser-driven targets have been observed with the Nova laser using 0.53 and 0.35 μm drive. The 0.35 μm drive produced larger modulations (equivalent to 3.3 μm rms surface finish) than 0.53 μm drive (2.0 μm rms). The laser intensity was $\sim 10^{13}$ W/cm², similar to that suggested for directly driven ignition targets during the first several ns. LASNEX simulations of this thermal smoothing effect in both the rms and spectrum agree with the 0.53 μm drive data, and are about 15% lower than the measured results with 0.35 μm drive. [S0031-9007(98)05453-2]

PACS numbers: 52.58.Ns

Successful implosion of a capsule by ablating the surface material (inertial confinement fusion or ICF) requires efficient energy absorption into the material. An obvious solution is to directly illuminate a pellet surface with laser light (or a particle beam). It has been recognized for some time that shorter wavelengths of laser light are more efficiently absorbed [1,2], and most of the research into direct drive fusion is currently concentrated in UV laser wavelengths, typically 0.35 μm (frequency tripled Nd glass) [3] or 0.25 μm (such as KrF) [4]. The problem with direct drive ICF is the difficulty of achieving the required uniformity of illumination; spatially nonuniform laser light leads to nonuniform ablation pressure, which produces a spatial modulation at the ablation surface (z_a). This surface is Rayleigh-Taylor unstable, and a modulation seeded by nonuniform laser light grows just as one seeded by an initial surface modulation [5]. It has been predicted [6] that laser nonuniformities will be smoothed by electron conduction (thermal smoothing) between the laser deposition surface (z_d) and the ablation surface, roughly as $\exp(-Dk)$, where k is the spatial wave number for a modulation and D is $z_d - z_a$. However, theory [7] also indicated that D is less for short laser wavelengths than for long; hence, the most efficient laser drive seeds the largest modulations and requires the most uniformity. Our experimental observations showed an increase in the modulations due to the drive when the laser wavelength is reduced.

We compared the modulations in areal density in a foil driven with either a 0.35 μm (blue) or a 0.53 μm (green) laser using one beam of the Nova laser. The drive beams were smoothed by random phase plates [8] (RPPs) which produced a well characterized, static spatial distribution for each color. We examined the modulations in each case at the shock transit time in order to eliminate the complication of Rayleigh-Taylor growth.

We performed our experiment in planar geometry (Fig. 1) to use the technique of time and space resolved radiography to infer variations in areal density in a foil from the modulation of a uniform x-ray backlighter. A

second beam of the Nova laser (also smoothed with a random phase plate) incident on a uranium foil produced the thermal x-ray backlighter. We made the driven foils of polyethylene (CH_2 , $\rho = 0.95$ g/cm³) 30 μm thick, mounted across a 750 μm diameter hole in a Mylar washer, and protected from low $h\nu$ x-ray flux from the backlighter by 12 μm of Be. The foils had an initial single-mode surface perturbation (50 μm wavelength and 2 μm initial amplitude) molded into the plastic on the driven side in order to calibrate the observed optical depth modulation due to drive laser speckle to an equivalent initial surface finish (Ref. [4]). We imaged the foils with a gated pinhole camera [9] using an array of 10 μm pinholes which produced twelve radiographs of the foil at different times, each with a duration of 100 ps. The uncertainty in absolute timing is about 200 ps. Because the two beams were opposed, it was not possible to view the foil exactly face on. The angle between the foil motion and the pinhole line of sight was 16° (no correction for this 4% distortion was made).

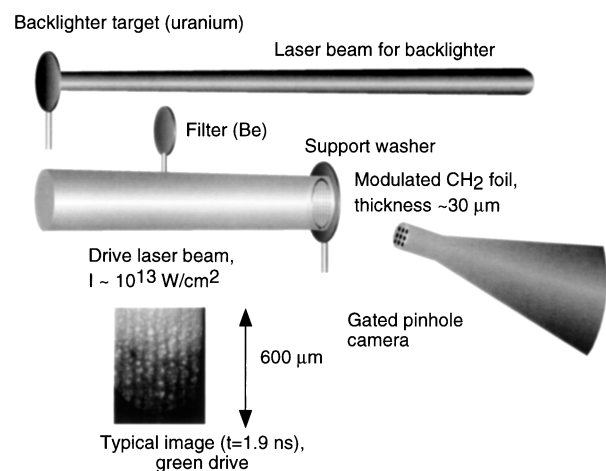


FIG. 1. Experimental configuration. The typical image shows the 50 μm wavelength calibration mode running vertically.

The images at $t = 1.9 \pm 0.2$ ns represent the imprint at the shock breakout time t_s . (There were five images from two separate shots for the $0.35 \mu\text{m}$ drive and four images from two shots for the $0.53 \mu\text{m}$ drive within 200 ps of this time.) After this time, Rayleigh-Taylor growth of the modulations is expected to dominate over any further imprint. We chose $300 \mu\text{m}$ square (in the object plane) sections of each image for analysis. We converted each frame to film exposure, removed the long scale length backlighter structure by dividing out a second order two-dimensional fit, removed the pure calibration mode at $50 \mu\text{m}$ with a numerical filter, and removed high-frequency noise with a parametric Wiener filter [10]. The negative of the natural logarithm of the result is equivalent to optical depth (τ), and because the opacity of the shock heated material is nearly cold opacity (at the backlighter peak $h\nu$ of 1 keV), the optical depth is proportional to areal density. The resulting square sections for two frames are shown in Figs. 2(a) and 2(b), contrasting blue (a) and green (b) drive. The two-dimensional power spectra (with mode zero at the center) were integrated for values of mode number $|m|$, i.e.,

$$P(m) = \int_0^{2\pi} [|T(|m|, \theta)|]^2 d\theta, \quad (1)$$

where P is the power spectrum, T is the Fourier transform of τ , $|m|$ is the magnitude of the mode number ($300 \mu\text{m}/\text{wavelength}$ in μm), and θ is the angle in Fourier space. When the Fourier transform is converted from Cartesian to polar coordinates, modes with $m - 0.5 < m \leq m + 0.5$ are taken to be mode m . The azimuthal integrals of the two-dimensional power spectra, averaged over all the frames, is shown on the left-hand axis in Fig. 3. It is preferable to make measurements of an imprint before nonlinear saturation effects complicate the interpretation of the calibration mode. We estimate the onset of nonlinear saturation to occur according to Haan [11] when the amplitude of the total modulation is greater than one-tenth of the wavelength. The conversion of optical depth modulation to spatial modulation may be estimated from the known (cold) opacity of the foil and the calculated density at t_s ($2.8 \text{ g}/\text{cm}^3$). Thus the 0.26 optical depth modulation for the $50 \mu\text{m}$ calibration mode is about $1.8 \mu\text{m}$ and, for the blue drive imprint between modes 4 and 8, 0.35 in optical depth is $2.5 \mu\text{m}$, for a total modulation of 3.1 (added in quadrature). Therefore we infer that around $50 \mu\text{m}$ (mode 6) the modulation is still linear. In addition, nonlinear effects are predicted [12] to become important when the amplitude of the second harmonic is approximately 0.3 times the amplitude of the fundamental. The amplitudes for the fundamental and second harmonic were 0.26 ± 0.03 and 0.04 ± 0.01 for a ratio of 0.15 (reduced from 0.25 by instrument blurring), so again we conclude the calibration wavelength is not significantly affected by saturation.

The laser pulse shape for these experiments was a 2 ns ramp from about 5×10^{12} to $1.5 \times 10^{13} \text{ W}/\text{cm}^2$ (to

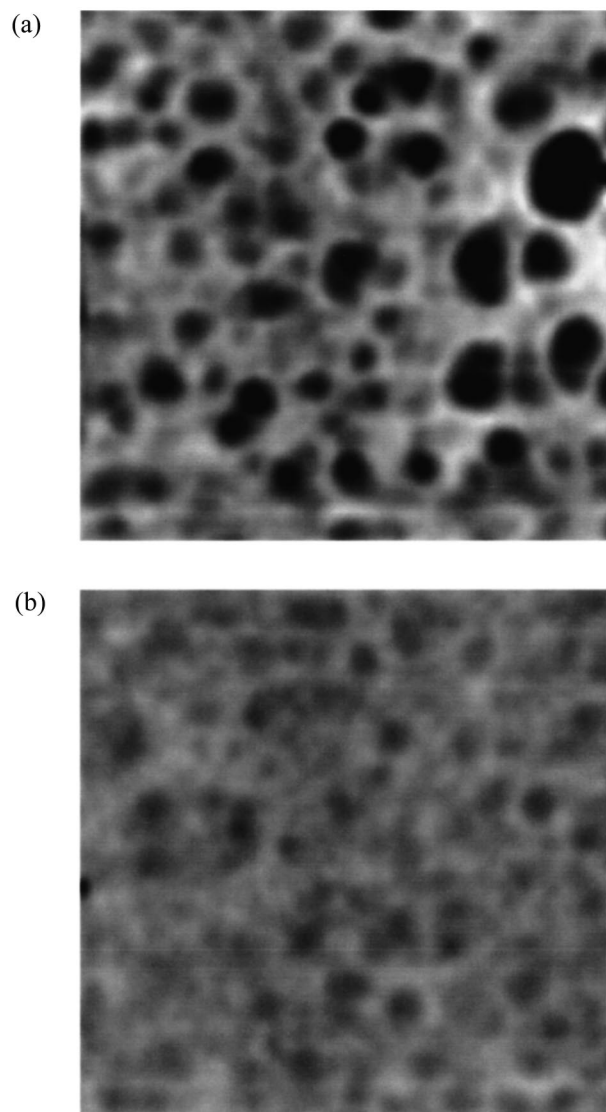


FIG. 2. Numerically processed radiographs of foils at shock breakout with (a) $0.35 \mu\text{m}$ light and (b) $0.53 \mu\text{m}$, both at $t = 1.8 \pm 0.2$ ns. The images are $300 \mu\text{m} \times 300 \mu\text{m}$; the gray scales are the same. The darker regions represent less areal density (bubbles).

$2 \times 10^{13} \text{ W}/\text{cm}^2$ for the green drive). The drive laser at $1.06 \mu\text{m}$ was either frequency doubled or tripled to produce the green or blue drive. We did not put additional bandwidth on the Nova laser (the pulse is transform limited with an inherent bandwidth of about $3 \times 10^{-4} \text{ THz}$), so the illumination patterns are fixed in time with a normalized standard deviation $[\sigma(I)/\langle I \rangle]$, where I is the intensity] of 1.0 in both cases. The characteristic speckle size of a laser beam with a circular near field illuminating an RPP is given by $2.44f\lambda$, where f is the f number of the focal lens and λ is the laser wavelength. The green beam was apertured to $f/11$ and smoothed with an RPP, giving a characteristic speckle size of $14 \mu\text{m}$ and a spot size of 1 mm . The blue beam was apertured

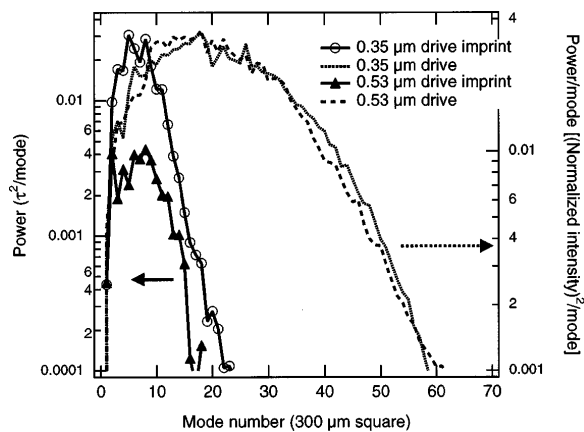


FIG. 3. Imprinted power spectra from radiographs for blue and green drive, shown in $(\text{optical depth})^2/\text{mode}$ (left axis), also, laser power spectra (right axis). Most of the laser power does not appear in the measured imprint.

to $f/15.6$ and smoothed with an RPP giving the same spot size and a speckle size of $13 \mu\text{m}$. (Had the same f number been used for both drives, the blue drive would have smaller characteristic speckles, which would undergo more thermal smoothing, thus reducing the observed blue imprint.) Both RPPs had hexagonal phase plate elements, with the elements 2 mm across for the blue drive and 3 mm across for the green. The (circular) laser spot produces round speckles, and the speckle pattern is isotropic for the two dimensions perpendicular to the foil motion. The two-dimensional power spectra of the laser speckle patterns and the imprint are thus azimuthally symmetric, so most of the information is contained in an azimuthal integral of the power spectrum. The azimuthal integrals of the power spectra of the speckle patterns (calculated in a similar fashion to the integrals of T), averaged over several $300 \mu\text{m}$ square regions, are plotted on the right-hand axis in Fig. 3. The power spectra for the two drive colors were essentially identical. Note that the theoretical spectral limit for the power spectrum is $f\lambda$, or mode 52 for the green and mode 55 for the blue.

In comparing the blue to green seeding, we were concerned that the increased efficiency (higher ablation pressure) of the blue drive might affect the growth during the shock transit ($t_s = 1.9 \text{ ns}$), resulting in a measurement which was dominated by different hydrodynamics of the two drive colors rather than the seeding. We simulated the experiment with one-dimensional LASNEX [13] and predicted the same shock transit time for the two drive colors at the measured irradiances. In addition, we examined the growth of the surface calibration modes, and found the same growth factor within experimental error, 2.4 ± 0.5 (blue) and 2.7 ± 0.4 (green). We concluded that the higher efficiency of the blue drive was compensated for by the higher intensity of the green drive.

The foil driven by the blue laser shows significantly more structure than the green. It is useful to define an

equivalent surface finish as the surface modulation which would have produced the same modulation in optical depth as the imprint produced. This may be determined from the $50 \mu\text{m}$ calibration mode by

$$\eta_{\text{eqs}}(k_x, k_y) = \frac{\eta_{\text{OD}}(k_x, k_y, t)}{\eta_{\text{OD}}(0, 2\pi/50, t)} \times 2 \mu\text{m}, \quad (2)$$

where η_{eqs} is the equivalent surface finish amplitude, $\eta_{\text{OD}}(k_x, k_y, t)$ is the measured modulation in optical depth at a given time and spatial frequency, $\eta_{\text{OD}}(0, 2\pi/50, t)$ is the measured modulation in optical depth of the $50 \mu\text{m}$ calibration mode, and $2 \mu\text{m}$ is the initial amplitude of the $50 \mu\text{m}$ calibration mode. This establishes the equivalence of the rms modulation (due to the laser imprint) to an initial surface rms in microns. For the blue drive this equivalent surface finish is $3.3 \pm 0.2 \mu\text{m}$ at the time of shock breakout and for the green it is $2.0 \pm 0.2 \mu\text{m}$. We simulated the imprint with two-dimensional LASNEX, using a $300 \mu\text{m}$ profile of the RPP smoothed beam. LASNEX predicted 2.8 and $1.7 \mu\text{m}$ equivalent surface finish for the blue and green drive. We attribute this increased imprinting of nonuniformities with blue drive as opposed to green to be caused by the reduced distance (D) between the mean laser deposition position and the ablation front for blue drive. Our LASNEX simulations predict that the difference between D for green to D for blue drive varies between $2 \mu\text{m}$ at 0.1 ns and $50 \mu\text{m}$ at 2 ns .

It is also useful to define an imprint efficiency for a given drive temporal history and material as the ratio of the imprinted equivalent surface in microns to the laser modulation in intensity. This imprint efficiency as a function of spatial wavelength is shown in Fig. 4. We simulated pure modes of sinusoidal laser modulation in LASNEX, and the derived imprint efficiencies for these modes are also shown in Fig. 4. In order to compare the data with the pure modes simulated in LASNEX, the data (measured imprint and measured laser modulation) were multiplied

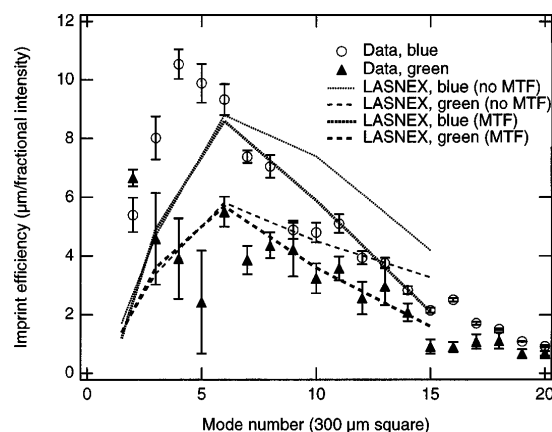


FIG. 4. Imprint efficiency for 0.35 and $0.53 \mu\text{m}$ drive, as measured and as predicted by LASNEX with and without instrument modulation transfer function.

by a Hanning window before taking Fourier transforms to avoid introducing artificial power from boundary discontinuities in the data. The fundamental mode at $300\ \mu\text{m}$ is then lost. The data show a peak in imprint efficiency near mode 4 for the blue drive, and appear to still be increasing at the lowest mode measured for the green drive. It is possible to introduce an artificial peak in the imprint efficiency if the instrument is incapable of resolving modulations at higher modes. The modulation transfer function (MTF) of the system is nearly Gaussian, dropping to 0.5 at mode 12 ($25\ \mu\text{m}$). The LASNEX simulations are shown both before and after convolution with the instrument MTF. The simulation convolved with the MTF agrees well with the data above mode 6. While LASNEX predicts the instrument MTF to reduce the observed efficiency at modes above about 10, the peak efficiency for both drive colors is not shifted and is simulated to be near mode 6 ($50\ \mu\text{m}$), with or without the instrument MTF.

The position of peak imprint efficiency is affected by two things, the creation of the rippled shock front by the laser modulation and the continuing evolution of the modulated shock front as it propagates through the material. As described above, the higher modes will be smoothed more effectively by the thermal smoothing, resulting in an imprint efficiency which is less for higher modes, and less overall for green than for blue drive. In addition, in the linear regime, the shock front amplitude has been shown [14] to oscillate, with phase inversion occurring when the foil thickness is approximately the same as the wavelength. The total areal density modulation measured here will thus show less growth for higher modes (shorter wavelengths). This effect should be the same for the blue drive as the green. We observe (for the blue drive) and simulate (for both) that the measured imprint efficiency increases with increasing mode number up to mode 4. This tendency has been described [15] to occur for wavelengths significantly longer than the separation of the absorption surface from the ablation front. For these wavelengths the increased material flow required to impart the same areal density modulation for a longer wavelength reduces the imprint efficiency. The slight discrepancy with LASNEX (the peak is observed at smaller modes for both the blue and green drive) may indicate that the energy is deposited at distances somewhat farther from the ablation surfaces than indicated by LASNEX.

In summary, we have observed the effect of varying the drive laser wavelength on the imprint in a plastic foil, and we see that shorter laser wavelengths do, in fact, produce more imprint. The imprint is equivalent in magnitude to a $3.3\ \mu\text{m}$ initial surface finish for blue

($0.35\ \mu\text{m}$) drive and to $2.0\ \mu\text{m}$ initial surface finish for green ($0.53\ \mu\text{m}$) drive. LASNEX gave a predicted value for the equivalent surface finish which was slightly lower than that observed. The imprint efficiency spectrum was found to decrease at shorter wavelengths in both cases due to thermal smoothing.

This work was performed under the auspices of the U.S. DOE by the Lawrence Livermore National Laboratory under Contract No. W-7405-ENG-48.

-
- [1] R. Fabbro, C. Max, and E. Fabre, *Phys. Fluids* **28**, 1463 (1985).
 - [2] M. H. Key *et al.*, *Phys. Fluids* **26**, 2011 (1983).
 - [3] J. M. Soares, R. L. McCrory, C. P. Verdon, A. Babushkin, R. E. Bahr, T. R. Boehly, R. Boni, D. K. Bradley, D. L. Brown, R. S. Craxton, J. A. Delettrez, W. R. Donaldson, R. Epstein, P. A. Jannimagi, S. D. Jacobs, K. Kearney, R. L. Keck, J. H. Kelly, T. J. Kessler, R. L. Kremens, J. P. Knauer, S. A. Kumpan, S. A. Letzring, S. J. Lonobile, S. J. Loucks, L. D. Lund, F. J. Marshall, P. W. McKenty, D. D. Meyerhofer, S. F. B. Morse, A. Okishev, S. Papernov, G. Pien, W. Seka, R. Short, M. J. Shoup III, M. Skeldon, S. Skupsky, A. W. Schmid, D. J. Smith, S. Swales, M. Wittman, and B. Yaakobi, *Phys. Plasmas* **3**, 2108 (1996).
 - [4] S. P. Obenschain, S. E. Bodner, D. Colombant, K. Gerber, R. H. Lehmburg, E. A. McLean, A. N. Mostovych, M. S. Pronko, C. J. Pawley, A. J. Schmitt, J. D. Sethian, V. Serlin, J. A. Stamper, C. A. Sullivan, J. P. Dahlburg, J. H. Garder, Y. Chan, A. V. Deniz, J. Hardgrove, T. Lehecka, and M. Klapisch, *Phys. Plasmas* **3**, 2098 (1996).
 - [5] S. G. Glendinning, S. N. Dixit, B. A. Hammel, D. H. Kalantar, M. H. Key, J. D. Kilkenny, J. P. Knauer, D. M. Pennington, B. A. Remington, R. J. Wallace, and S. V. Weber, *Phys. Rev. E* **54**, 4473 (1996).
 - [6] S. E. Bodner, *J. Fusion Energy* **1**, 221 (1981).
 - [7] H. A. Baldis, E. M. Campbell, and W. L. Kruer, in *Laser-Plasma Interactions*, edited by M. N. Rosenbluth and R. Z. Sagdeev, *Handbook of Plasma Physics* Vol. 3 (Elsevier, New York, 1991), Chap. 9.
 - [8] S. N. Dixit *et al.*, *Appl. Opt.* **32**, 2543 (1993).
 - [9] J. D. Kilkenny, *Laser Part. Beams* **9**, 49 (1991).
 - [10] R. C. Gonzalez and P. Wintz, *Digital Image Processing* (Addison-Wesley, Reading, Massachusetts, 1977), Chap. 5.
 - [11] S. Haan, *Phys. Rev. A* **39**, 5812 (1989).
 - [12] J. W. Jacobs and I. Catton, *J. Fluid Mech.* **187**, 329 (1988); **187**, 353 (1988).
 - [13] G. B. Zimmerman and W. L. Kruer, *Comments Plasma Phys. Controlled Fusion* **2**, 51 (1975).
 - [14] T. Endo *et al.*, *Phys. Rev. Lett.* **74**, 3608 (1995).
 - [15] J. P. Dahlburg *et al.*, *Bull. Am. Phys. Soc.* **40**, 1750 (1995).